e-ISSN: 2149-7826

journal.phaselis.org

PHASELIS | Disiplinlerarası Akdeniz Araştırmaları Dergisi
Journal of Interdisciplinary Mediterranean Studies

Issue IX (2023)

Coastal Geomorphology and Coastal Erosion of Phaselis Ancient City and its Surroundings

Phaselis Antik Kenti ve Çevresinin Kıyı Jeomorfolojisi ve Kıyı Erozyonu

Ebru AKKÖPRÜ
https://orcid.org/0000-0001-8751-7771

Musa TAŞ
https://orcid.org/0000-0002-6243-7713

Citation Akköprü E. & Taş M. 2023, "Coastal Geomorphology and Coastal Erosion of Phaselis Ancient City and its Surroundings". *Phaselis* IX, 51-63.
https://doi.org/10.5281/zenodo.10407367

Received Date: 06.09.2023 | Acceptance Date: 27.11.2023
Online Publication Date: 19.12.2023

Editing Phaselis Research Project
www.phaselis.org

PHASELIS

Geliş Tarihi: 06.09.2023
Kabul Tarihi: 27.11.2023
Yayın Tarihi: 19.12.2023

IX (2023) 51-63
DOI: 10.5281/zenodo.10407367
journal.phaselis.org

Coastal Geomorphology and Coastal Erosion of Phaselis Ancient City and its Surroundings

Phaselis Antik Kenti ve Çevresinin Kıyı Jeomorfolojisi ve Kıyı Erozyonu

Ebru AKKÖPRÜ* & Musa TAŞ**

Abstract: The aim of this study is the detection of coastal changes in and around the ancient city of Phaselis between the years 1957, 1981, 1992, 2009 and 2019. A literature review was carried out and it was determined that the Digital Shoreline Analysis System (DSAS) was the most appropriate method for detecting coastal change. DSAS, an extension of the ArcGIS program, is a method that effectively calculates changes in coastal shorelines from past years. In this study, the most preferred statistical analyses within the DSAS analysis method were used, including Net Shoreline Movement (NSM), End Point Rate (EPR), and Shoreline Change Envelope (SCE). While the DSAS method often relies on Landsat satellite imagery, in this study, aerial photographs from the General Directorate of Mapping (HGM) were used, providing more detailed data for the years 1957, 1981, 1992, 2009, and 2019. The reason for not using Landsat satellite images is that the study area covers a small geographical area. This limitation prevents Landsat satellite imagery from providing a detailed view. During the analyses, the study area was divided into four sections: Bostanlık Bay, City Harbor, Northern Harbor and Cennet Bay. Bostanlık Bay was further divided into two parts, labelled A and B, for investigation. The results of the analyses showed that sedimentation occurred in certain areas of the ancient city of Phaselis and its surroundings. In other areas, erosion occurred. The occurrence of sedimentation is attributed to both natural processes and anthropogenic activities. The most prominent example of anthropogenic activity can be seen along the coast of Cennet Bay.

Keywords: Phaselis, Coast, Coastal Erosion, Dsas, Cbs

Öz: Bu çalışmanın amacı Phaselis Antik Kenti ve çevresinin 1957, 1981, 1992, 2009 ve 2019 yılları arasındaki kıyı değişimini ortaya koymaktır. Yapılan literatür çalışması sonucunda kıyı değişimini tespit etmek için en uygun yöntemin Digital Shoreline Analysis System (DSAS/Dijital Kıyı Çizgisi Analiz Sistemi) olduğu tespit edilmiştir. ArcGIS programının bir uzantısı olarak kullanılan DSAS, geçmiş yıllara ait kıyı şeridi değişimlerini en uygun biçimde hesaplayan bir yöntemdir. DSAS analiz yöntemi içinde en çok tercih edilen istatistik analizleri olan Net Kıyı Hareketi/Net Shoreline Movement (NSM), Bitiş Noktası Oranı/End Point Rate (EPR) ve Kıyı Şeridi Değiştirme Zarfı/ Shoreline Change Envelope (SCE) bu çalışmada kullanılmıştır. DSAS yöntemi uygulanırken daha çok Landsat uydu görüntülerinden yararlanılır. Ancak bu çalışmada daha ayrıntılı veri sağlayan Harita Genel Müdürlüğü'nden (HGM) temin edilmiş olan 1957, 1981, 1992, 2009 ve 2019 yıllarına ait hava fotoğrafları kullanılmıştır. Landsat uydu görüntüsünden yararlanmamanın nedeni çalışma alanın küçük bir sahayı kapsamasıdır. Bu da Landsat uydu görüntülerinin ayrıntılı bir görüntü almasına engel olmaktadır. Analizler yapılırken çalışma alanını Bostanlık Koyu, Kent Limanı, Kuzey Limanı ve Cennet Koyu olarak dört bölüme ayırılmıştır. Bostanlık Koyu kendi içerisinde A ve B olarak iki kısımda incelenmiştir. Yapılan analizler sonucunda ise Phaselis Antik Kenti ve çevresinin belli alanlarda birikme olurken belli alanlarında ise erozyon meydana gelmiştir. Birikme olayının gerçekleşmesinin nedeni doğal süreçlerin yanı sıra antropojen faaliyetlerdir. Antropojenik faaliyetlerin en iyi örneğini ise Cennet Koyu kıyılarında görülür.

Anahtar sözcükler: Phaselis, Kıyı, Kıyı Erozyonu, Dsas, Cbs

* Doç. Dr., Akdeniz Üniversitesi, Edebiyat Fakültesi, Coğrafya Bölümü, Antalya. ebruakkopru@akdeniz.edu.tr | https://orcid.org/0000-0001-8751-7771

** MA, Akdeniz Üniversitesi, Sosyal Bilimler Enstitüsü, Coğrafya Anabilim Dalı, Antalya. mtas12599@gmail.com | https://orcid.org/0000-0002-6243-7713

Article Type: Research | Received Date: 06.09.2023 | Acceptance Date: 27.11.2023 ; Akköprü E. & Taş M. 2023, "Coastal Geomorphology and Coastal Erosion of Phaselis Ancient City and its Surroundings". *Phaselis* IX, 51-63.

Introduction

Coasts, which are pieces of land bordering the sea, have been important living spaces for living creatures, especially humans, throughout history. Coastal areas have been and still are used for shelter, industry, agriculture, tourism, natural and cultural resources and recreational activities throughout the historical development process[1]. Phaselis Ancient City is situated 50 km away from Antalya, located at approximately 36°52' north latitude and 27°55' east longitude. It falls within the borders of the Tekirova neighborhood in the Kemer district[2] (Fig. 1). The study area's boundaries were established by considering the watershed formed by small streams that supply water to Phaselis Ancient City and flow into the sea or the Asar Lagoon. Accordingly, it starts from the south of Çamyuva neighborhood in the north and ends with the alluvial plain formed by the Karaçay Stream in the southwest (Fig. 1). Phaselis Ancient City was established on two distinct geographical surfaces that are separated from each other: the cape extending towards the sea, and the settlement area on the hill and its foothills to the north[3,4].

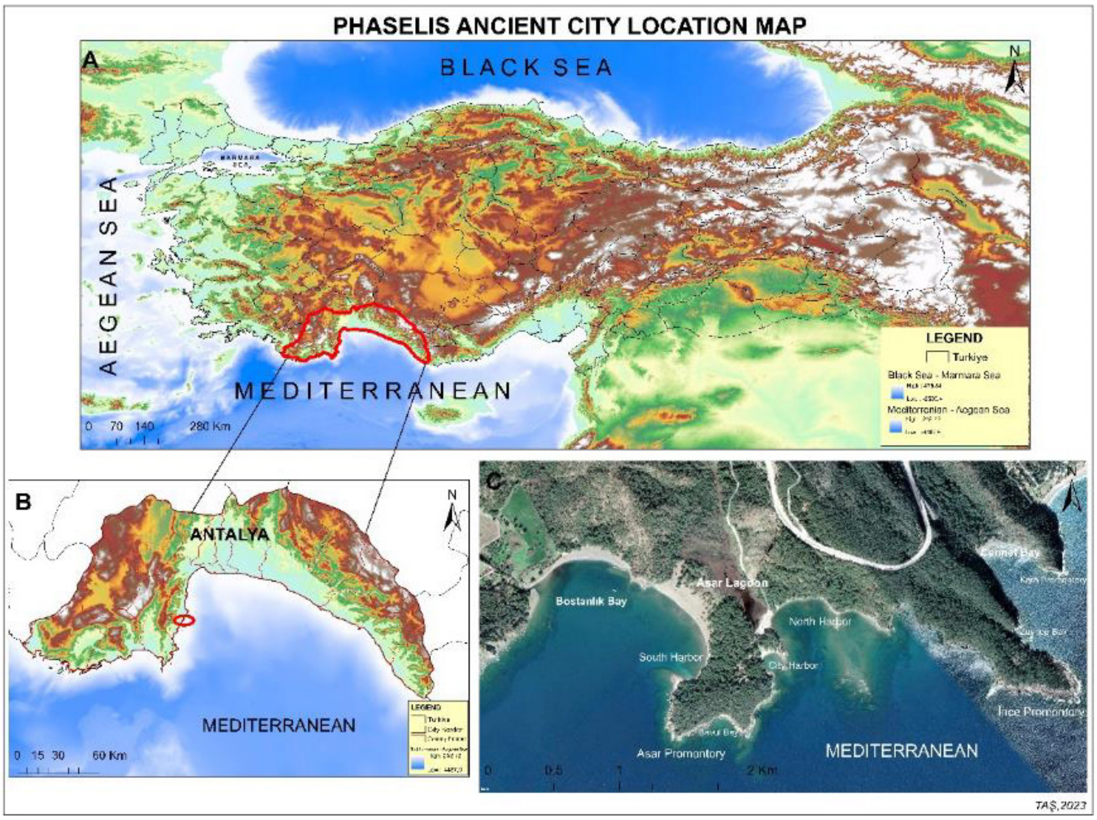

Fig. 1. Phaselis Ancient City Location Map. A: The location of Antalya province on the physical geography map of Türkiye. B: Location of Phaselis Ancient City on the physical geography map of Antalya province. C: Top view of Phaselis Ancient City

From a morphological perspective, Phaselis Ancient City and its surroundings are distinguished by the presence of elevated hills, which are part of the Tahtalı Mountains range. The central area of

1 Döker 2012, 1351.
2 Akköprü 2022, 224.
3 Atasoy 2010, 50.
4 Öner 2018, 352.

the city is home to the Asar Lagoon[5], now covered with swamps and reeds. The Asar Lagoon is nourished by several small seasonal streams, with the Gökgür Stream being particularly notable. Another significant geomorphological feature of Phaselis Ancient City is the tombolo, upon which many important structures, including the theater and acropolis, were constructed. Along the coastal section of the tombolo, cliffs dominate, while in the inner part, there are two hills rising to heights of 55 meters and 60 meters.To the north of the tombolo, you'll find both city harbor and Northern Harbor. Asar Lagoon lies to the west, Bavul Bay to the east, and to the south, there are both Southern Harbor and Bostanlık Bay. To the north of the tombolo, you'll find both city Harbor and Northern Harbor. Asar Lagoon lies to the west, Bavul Bay to the east, and to the south, there are both Southern Harbor and Bostanlık Bay[6] (Fig. 2).

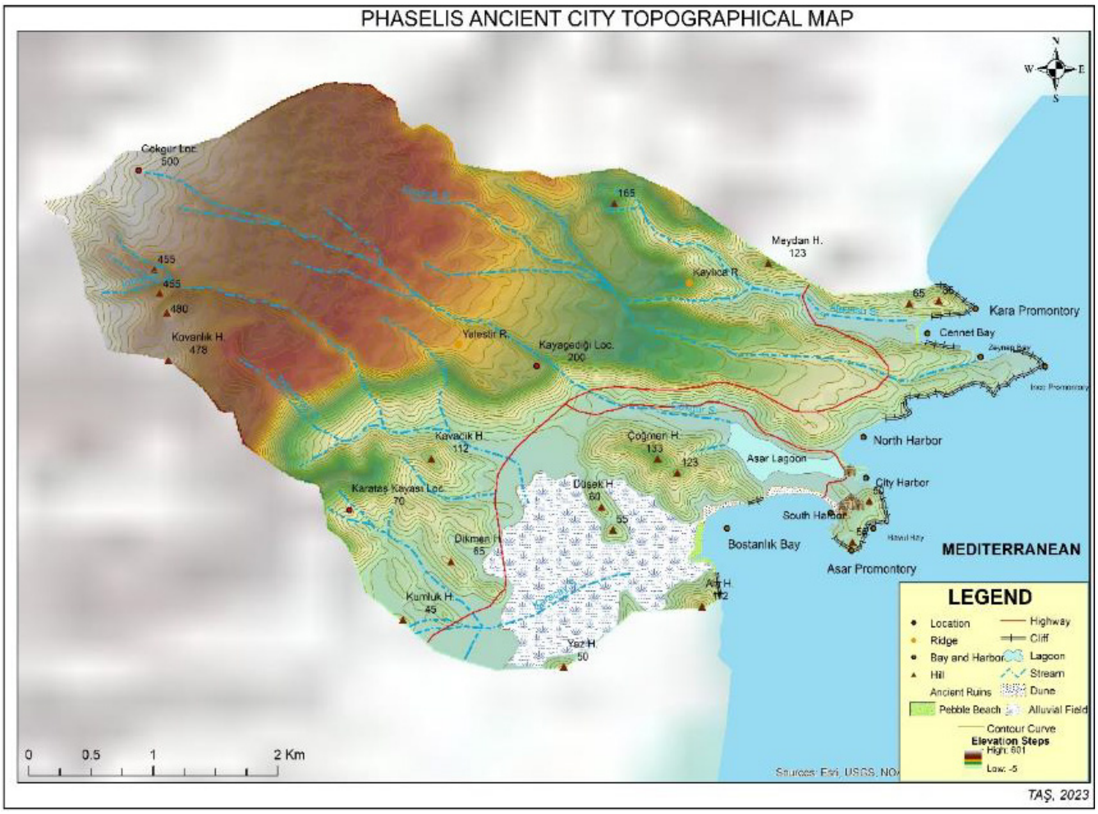

Fig. 2. Phaselis Ancient City Topography Map

Phaselis and its environs boast bays of varying sizes, owing to their intricately indented coastlines. Vast coastal dunes extend behind these formed bays. Furthermore, significant ports were established within these bays, bestowing upon Phaselis the distinction of being a port city.

When discussing the hydrography of Phaselis and its surroundings, Schafer (1981) references a water source that held significant importance in the founding of the ancient city[7]. Within the study area, numerous seasonal streams of varying sizes flow into lagoons and bays (Fig. 3). Gökgür Stream, which feeds into Asar Lagoon, originates between the Kocain cliffs at an elevation of 500 meters and Gökgür Locality (Fig. 3). Karaçay Stream, which flows into the alluvial plain to the west of Bostanlık Bay, originates from multiple locations. Kirsecik Stream empties into Zeynep Bay, situated in the

[5] For lagoon borders see also Arslan & Tüner Önen 2021, 156.

[6] Aslan & Orhan 2019, 85-99.

[7] Schafer 1981, 30.

northern part of İnce Promontory. Within this region, sedimentary materials transported by the stream have accumulated. Alacasu Stream, coursing toward Cennet Bay, takes its source from three different points, amassing the materials it carries in this area, thus forming a sandy-pebble beach.

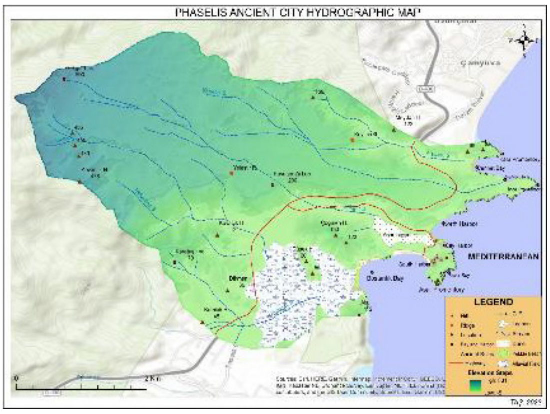

Fig. 3. Phaselis Ancient City Hydrographic Map

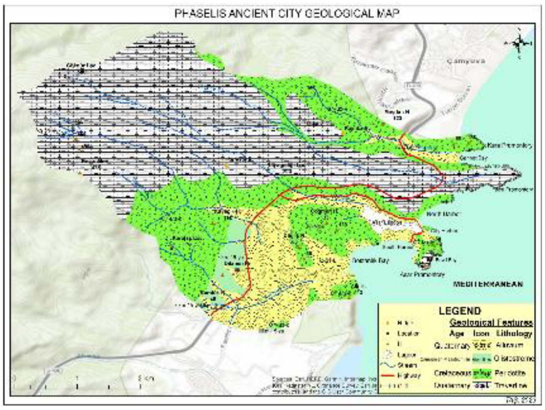

Fig. 4. Phaselis Ancient City Geological Map[8]

To briefly discuss the geology of Phaselis and its surroundings, the northern slopes of the Ancient City are cloaked with quaternary-aged travertines. These travertines, which overlay Cretaceous-aged peridotites, stretch from an altitude of 400 meters down to sea level. In contrast, the southern regions of İnce Promontory comprise Cretaceous-aged peridotites, while the northern areas are characterized by quaternary-aged travertines. The area behind Cennet Bay is primarily dominated by quaternary alluviums. Kara Cape is situated on Cretaceous-aged peridotites (Fig. 4). The Phaselis tombolos are comprised of Cretaceous-aged peridotites. Çoğmen Hill (133 meters) and Düşek Hill (60 meters), located just west of Asar Lagoon, are covered with Cretaceous-aged peridotites, while their surroundings are adorned with quaternary-aged alluviums transported by streams. The southern and western slopes of Kavacık Hill (112 meters), found in the interior, are mainly characterized by ophiolitic flysch (olistostrome) lithology. The upper regions of Kavacık Hill consist of gabbro and diabase (peridotite)[9] (Fig. 4).

Material and Method

After conducting a thorough literature review, it was determined that the most precise and effective method for assessing coastal changes in the Ancient City of Phaselis and its vicinity is the DSAS (Digital Shoreline Analysis System). The DSAS tool serves as an extension within the ArcGIS program. This method accurately computes coastal changes by comparing historical coastlines of the area over time. Although Landsat satellite images are commonly used when employing the DSAS approach (see Kuleli 2010, Döker 2012, Özpolat & Demir 2014, Topuz 2018, Kılar & Çiçek 2018), this study utilized aerial photographs from 1957, 1981, 1992, 2009, and 2019, sourced from the General Directorate of Mapping (HGM), providing more detailed and comprehensive data.

The DSAS method, originally developed by the United States Geological Survey (USGS) in the early 1990s, is a computer software program based on Geographic Information Systems (GIS). DSAS offers the capability to conduct various data analyses. When deemed appropriate, statistical analysis methods such as NSM, SCE, and EPR are employed for effectiveness.

The Net Shoreline Movement (NSM) statistical method is not designed to calculate the rate or

8 Akköprü *et al.* 2022, 227.
9 Akköprü *et al.* 2022, 227.

speed of shore change. Instead, it measures the distance in meters between the shorelines of two specific dates, typically the oldest and the most recent ones[10] (Fig. 5).

The Shoreline Change Envelope (SCE) statistical method calculates a distance in meters, rather than a ratio. The SCE value is instrumental in identifying the greatest distance between all coastlines intersecting a specific section. In simpler terms, it measures the distance between the most advanced shoreline of a coastline and the most retreated shoreline, as depicted in Figure 5.

The End Point Rate (EPR) statistical method is determined by dividing the distance of coastline movement by the time that has passed between the oldest and newest coastlines. In essence, the End Point Rate is calculated by dividing the Net Shoreline Movement by the elapsed time (Fig. 5). The End Point Rate (EPR) method offers several key advantages, including its simplicity of calculation and the utilization of data from only two specific coastline dates during the calculation process. However, a notable disadvantage is that it may overlook additional information when more comprehensive data is at hand[11].

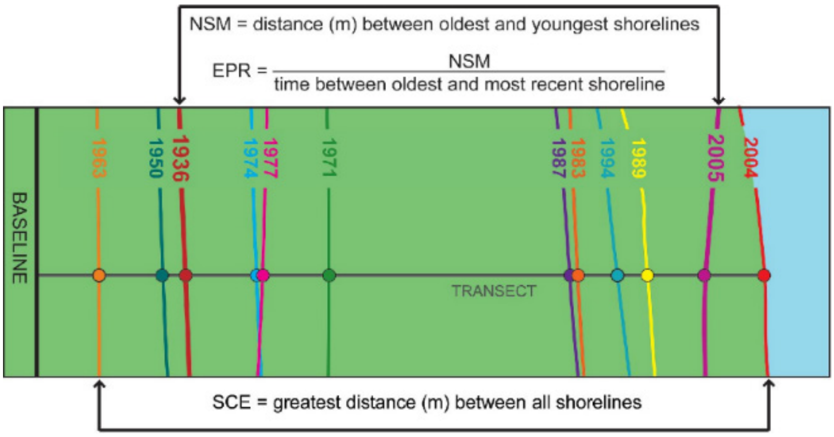

Fig. 5. Illustration of NSM, EPR and SCE statistical analyses[12]

Findings

In this study, the Ancient City of Phaselis was examined within four distinct groups: Bostanlık Bay (which was further divided into A and B sections), City Harbor, Northern Harbor, and Cennet Bay. Coastal changes in each of these areas were investigated by conducting NSM, EPR, and SCE analyses. In the subsequent section, the analysis results for the respective coastlines are presented and discussed under specific headings.

Changes on the Shores of Bostanlık Bay

Bostanlık Bay NSM Analysis Results

Along the shores of Bostanlık Bay (Section A), measurements were taken from 38 points at 10-meter intervals as per NSM statistics. For NSM analysis, the oldest available shoreline data from 1957 and the most recent data from 2019 were utilized. Comparing the shorelines between 1957 and 2019, the most substantial accumulation was observed in section 32, with an increase of 18.97 meters. Conversely, the highest erosion was recorded in section 2, with a decrease of -2.27 meters. Notably, along the coast of Bostanlık Bay (Section A), coastal changes predominantly occurred in the direction of accumulation (Fig. 6a-b).

---

[10] Himmelstoss *et al.* 2018, 48; Dolan *et al.* 1991, 724-725.

[11] Himmelstoss *et al.* 2018, 48.

[12] Himmelstoss *et al.* 2018, 51.

As per NSM statistics, a total of 154 sections were surveyed at 10-meter intervals along the coast of Bostanlık Bay (Section B). For this analysis, data from the years 1957 and 2019 were compared.

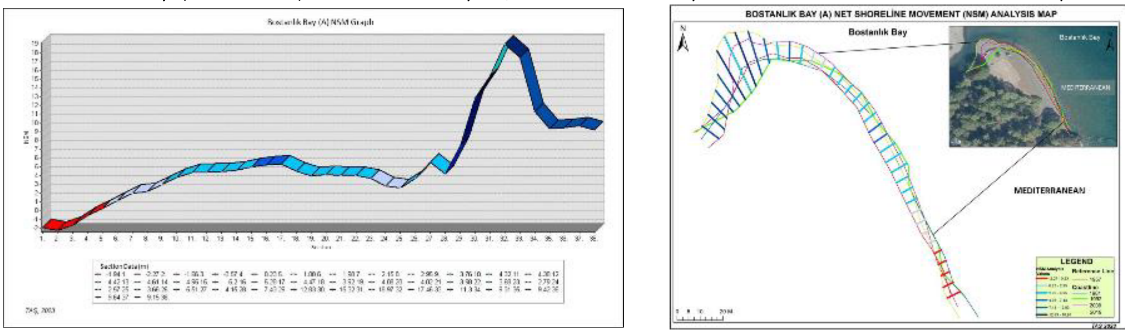

Fig. 6a-b. Bostanlık Bay A NSM graph (a). Bostanlık Bay A NSM map (b)

The most significant erosion was observed in section 124, with a substantial decrease of -17.57 meters. Conversely, the highest accumulation was identified in section 25, with an increase of 7.22 meters (Fig. 7a-b). In the area encompassing the cliff situated in the middle of Bostanlık Bay (Section B), it has been observed that accumulation predominantly characterizes the southern side of the cliff. Conversely, erosion has been identified on the northern side of the cliff, specifically within the region housing the South Port. Remarkably, there has been minimal erosion within the vicinity of the cliff itself (Fig. 7a-b).

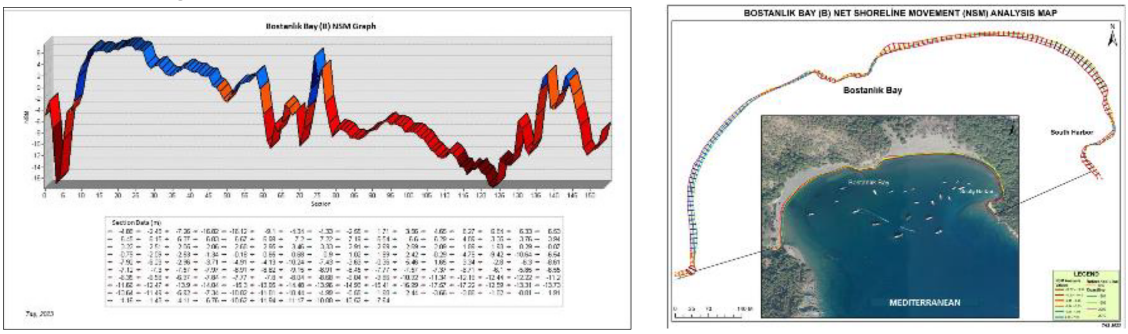

Fig. 7a-b. Bostanlık Bay B NSM graph (a). Bostanlık Bay B NSM map (b)

Bostanlık Bay EPR Analysis Results

Along the shores of Bostanlık Bay (Section A), measurements were collected from 38 points at 10-meter intervals, following EPR statistics. For the EPR analysis, data from the earliest coastline in 1957 and the most recent coastline in 2019 were employed.

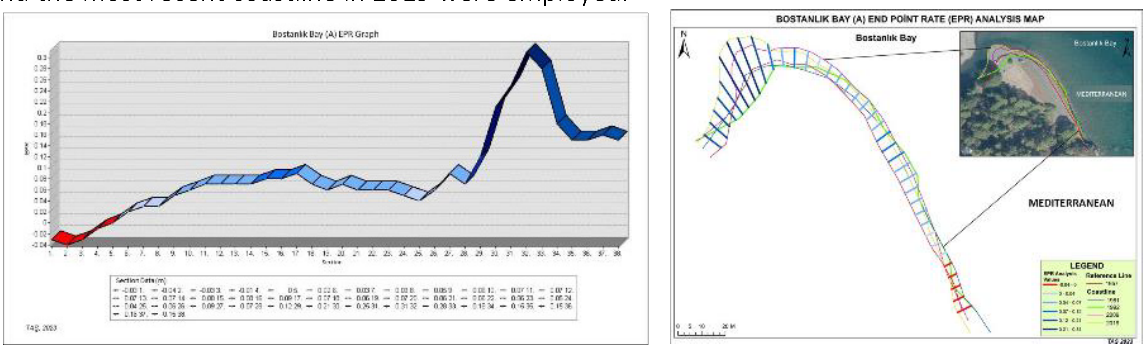

Fig. 8a-b. Bostanlık Bay A EPR graph (a). Bostanlık Bay A EPR map (b)

Over the 62-year period spanning these years, the section exhibiting the most substantial accumulation was identified as section 32, with an annual accumulation rate of 0.31 meters. In contrast, the highest level of erosion was observed in section 2, where the annual erosion rate was -0.04 meters (Fig. 8a-b). In this area, a prevailing trend of accumulation has been noted, with minimal erosion almost absent.

Based on the outcomes of the EPR analysis along the coast of Bostanlık Bay (Section B), data was gathered from 154 points at 10-meter intervals. Over the 62-year period between 1957 and 2019, the most substantial erosion was documented in section 124, with an annual erosion rate of -0.28 meters. Conversely, the highest accumulation was observed in section 25, with a maximum rate of 0.12 meters per year (Fig. 9a-b).

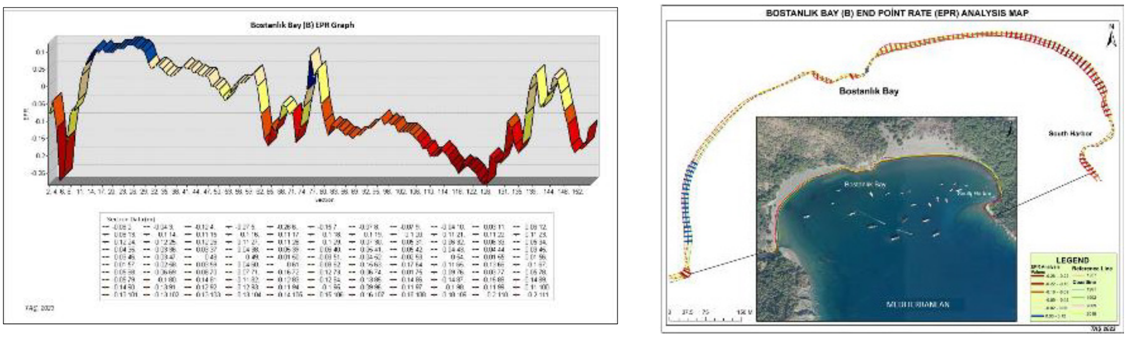

Fig. 9a-b. Bostanlık Bay B EPR graph (a). Bostanlık Bay B EPR map (b)

Bostanlık Bay SCE Analysis Results

According to the results of the SCE analysis, data was collected from 38 points at 10-meter intervals along the shores of Bostanlık Bay (Section A). The most significant coastal change on the coast of Bostanlık Bay (Section A) was recorded between 1992 and 2019, with a change of 27.11 meters observed in section 32 (as depicted in Fig. 10a-b). In section 32 of Bostanlık Bay (Section A), an accumulation of 2.03 meters was observed between 1957 and 1981. However, between 1981 and 1992, this area experienced a substantial erosion of -10.27 meters. From 1992 to 2019, a distinct accumulation pattern dominated (Fig. 10a-b).

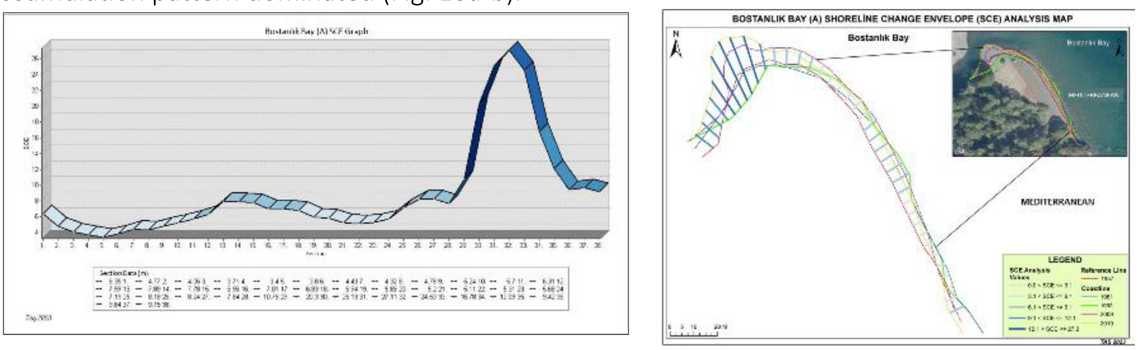

Fig. 10a-b. Bostanlık Bay A SCE graph (a). Bostanlık Bay A SCE map (b)

According to the results of the SCE analysis, data was collected from 154 points at 10-meter intervals along the shores of Bostanlık Bay (Section B). The most significant coastal change was observed in section 124, as shown in Fig. 11a-b. This area underwent a substantial change of 18.61 meters between 1957 and 2009. In the specific location of section 124, continuous erosion occurred over this period (-18.61 meters) from 1957 to 2009. However, a subsequent accumulation of 1.04 meters was documented between 2009 and 2019 (Fig. 11a-b).

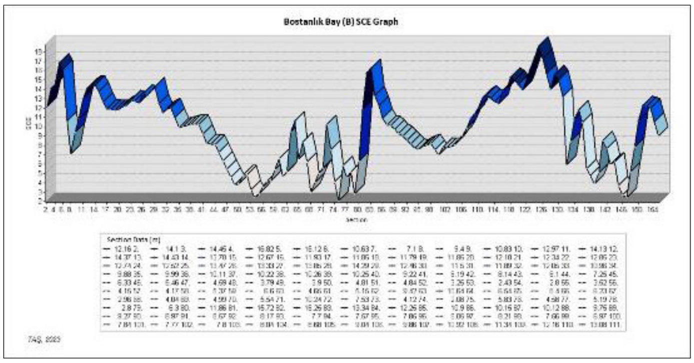

a

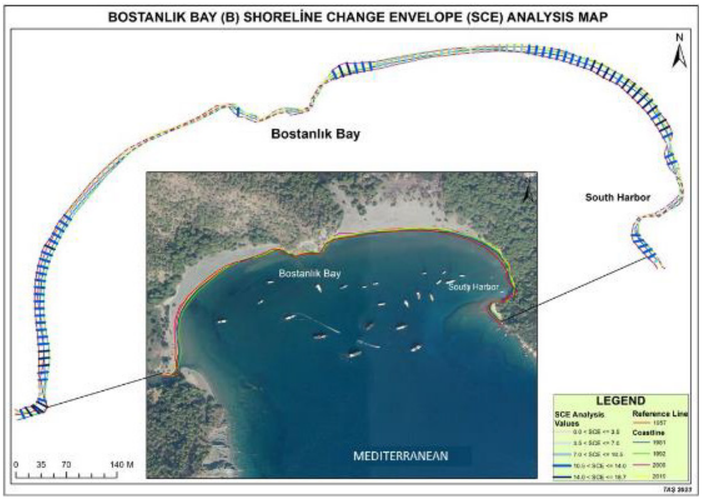

b

Fig. 11a-b. Bostanlık Bay B SCE graph (a). Bostanlık Bay B SCE map (b)

Changes on the City Harbor Shore

City Harbor NSM Analysis Results

To conduct the NSM analysis in the vicinity of the City Port, 29 sections were surveyed at 10-meter intervals. In this analysis, the earliest available data from 1957 was compared with the most recent data from 2019. The findings revealed that the most significant accumulation occurred in section number 8, with a substantial increase of 10.31 meters, as depicted in Fig. 12a-b. Conversely, the highest erosion was identified in section 28, with a decrease of -4.55 meters. Notably, accumulation predominantly characterized the southern side of the City Port, while erosion prevailed on the northern side, as illustrated in Fig. 12a-b.

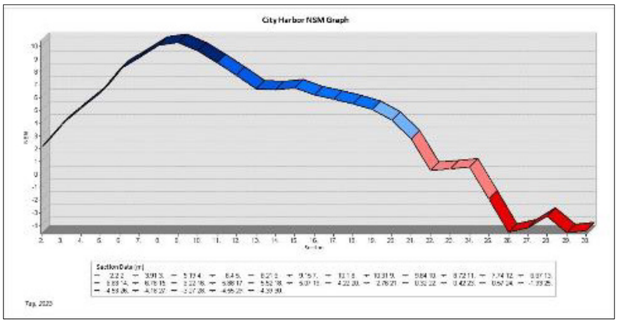

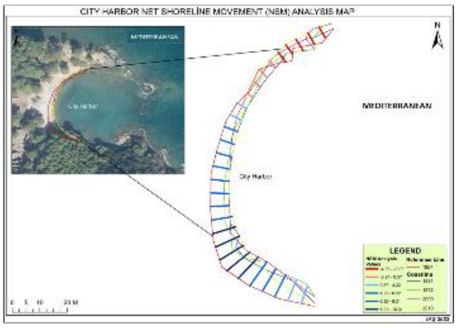

Fig. 12a-b. City Harbor NSM graph (a). City Harbor NSM map (b)

City Harbor EPR Analysis Results

To perform the EPR analysis of the City Port, data was collected from 29 points at 10-meter intervals. The EPR analysis utilized data from 1957 (the oldest data) and 2019 (the most recent data). Based on the results of the EPR analysis, over the 62-year period spanning 1957 to 2019, the highest accumulation rate was recorded in section 8, with a rate of 0.17 meters per year, as depicted in Fig. 13a-b. In contrast, the maximum annual erosion rate between 1957 and 2019 was observed in section 28, reaching -0.7 meters per year (Fig. 13a-b).

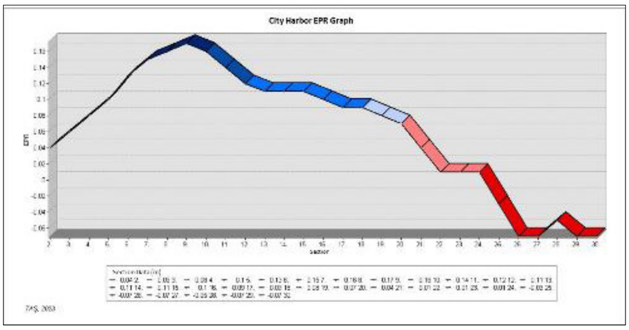

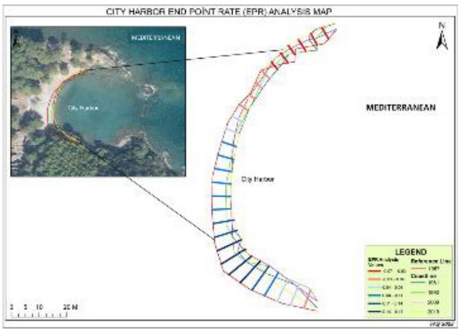

Fig. 13a-b. City Harbor EPR graph (a). City Harbor EPR map (b).

City Harbor SCE Analysis Results

In the SCE analysis of the City Port, data was collected from 29 points at 10-meter intervals. The most substantial change was observed in section number 5, with a change of 10.8 meters documented between 1957 and 2009 (Fig. 14a-b). The coastal area where section 5 is situated reached its lowest point in 1957. Starting from 1957 and extending to 2009, this area began to progressively accumulate towards the sea. However, from 2009 to 2019, the region encompassing section number 5 experienced erosion, with a total loss of -2.59 meters during that period (Fig. 14a-b).

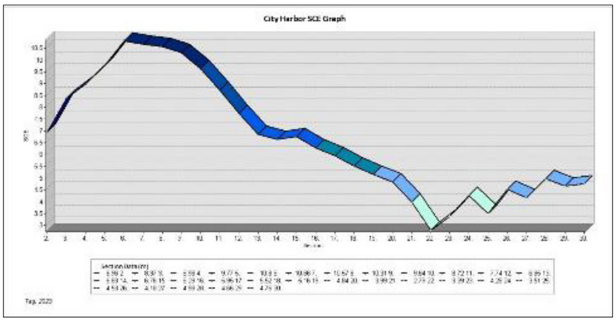

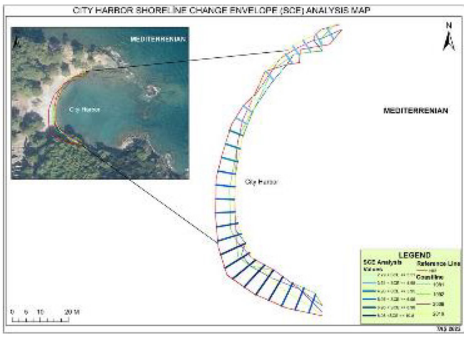

Fig. 14a-b. City Harbor SCE graph (a). City Harbor SCE map (b).

Changes on the North Harbor Shore

North Harbor NSM Analysis Results

To conduct the NSM analysis in the area previously designated as the North Port, data was gathered from 89 points at 10-meter intervals. The NSM analysis employed data from 1957 (the oldest data) and 2019 (the most recent data). The analysis revealed that the most significant accumulation was observed in the region corresponding to section number 2, with an increase of 11.79 meters when comparing the data from 1957 to 2019 (Fig. 15a-b). The most substantial erosion was identified in the region associated with section number 55, totaling -11.12 meters. Notably, accumulation predominantly characterized the southern side of the North Port, whereas the northern side experienced more pronounced erosion activity (Fig. 15a-b).

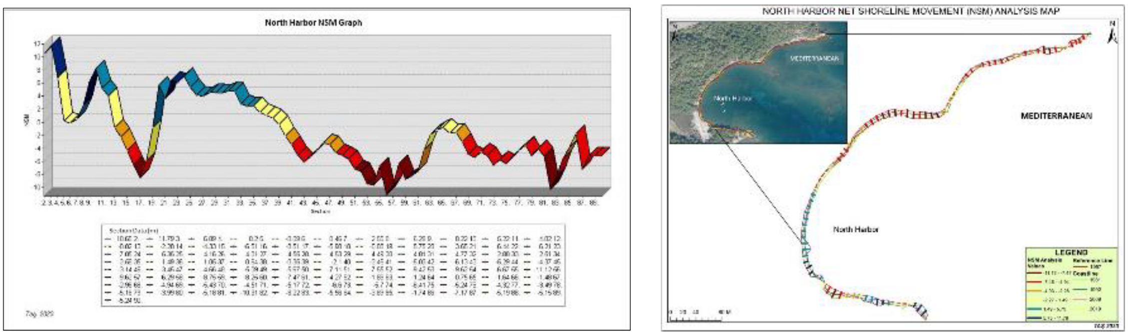

Fig. 15a-b. North Harbor NSM graph (a). North Harbor NSM map (b).

North Harbor EPR Analysis Results

To conduct the EPR analysis in the North Port, data was collected from 89 points at 10-meter intervals. The EPR analysis employed data from 1957 (the oldest coastline) and 2019 (the newest coastline). Based on the EPR analysis, over the 62-year period spanning 1957 to 2019, the highest accumulation rate in the North Port was found to be 0.19 meters per year in section number 2, as depicted in Fig. 16a-b. Conversely, the maximum erosion rate between 1957 and 2019 was observed in section 55, with a rate of -0.18 meters per year, as shown in Fig. 16a-b.

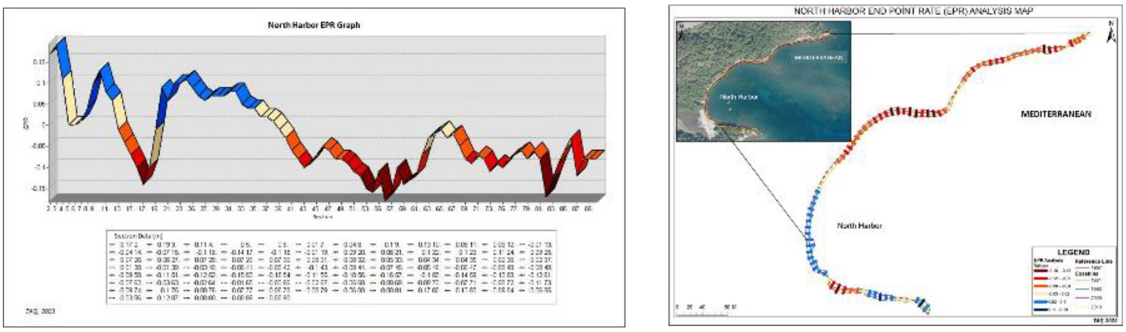

Fig. 16a-b. North Harbor EPR graph (a). North Harbor EPR map (b).

North Harbor SCE Analysis Results

In the SCE analysis of the North Port, data was gathered from 89 points at 10-meter intervals. The analysis unveiled that the most substantial change on the coast was observed in section 16, with a change rate of 13.24 meters, as shown in Fig. 16a-b. The area encompassing section 16 experienced a significant erosion of -13.24 meters over the 24-year period between 1957 and 1981. Subsequently, an accumulation of 4.71 meters was documented over the 38-year period from 1981 to 2019 (Fig. 16a-b).

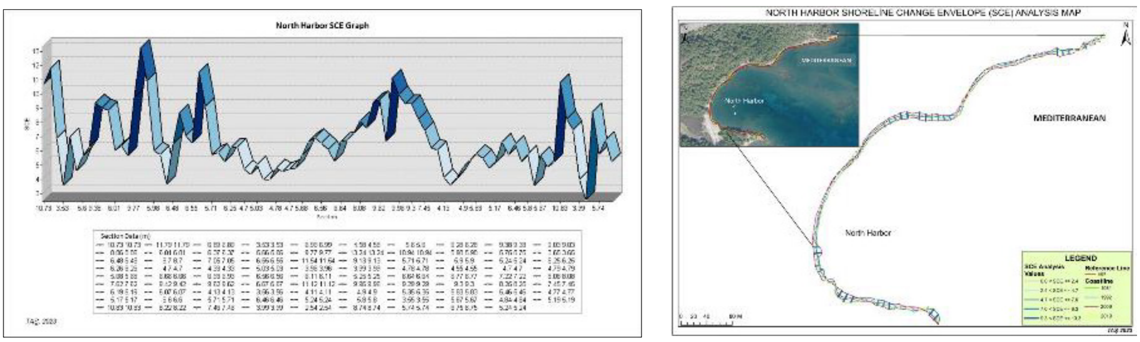

Fig. 17a-b. North Harbor SCE graph (a). North Harbor SCE map (b).

Changes to Cennet Bay Beach

Cennet Bay NSM Analysis Results

To obtain the results of the NSM analysis for Cennet Bay, situated between İnce Promontory and Kara Promontory in the northern part of Phaselis, measurements were obtained from 21 points at 10-meter intervals. The NSM analysis incorporated data from 1957 (the oldest data) and 2019 (the most recent data). Upon comparing the data from 1957 to 2019, the most substantial accumulation was identified in the region corresponding to section 21, exhibiting an increase of 12.87 meters (Fig. 18a-b). Cennet Bay has experienced minimal erosion. Over the 62-year period, the most notable erosion was observed in the region associated with section 17, with a decrease of -1.34 meters (Fig. 18a-b).

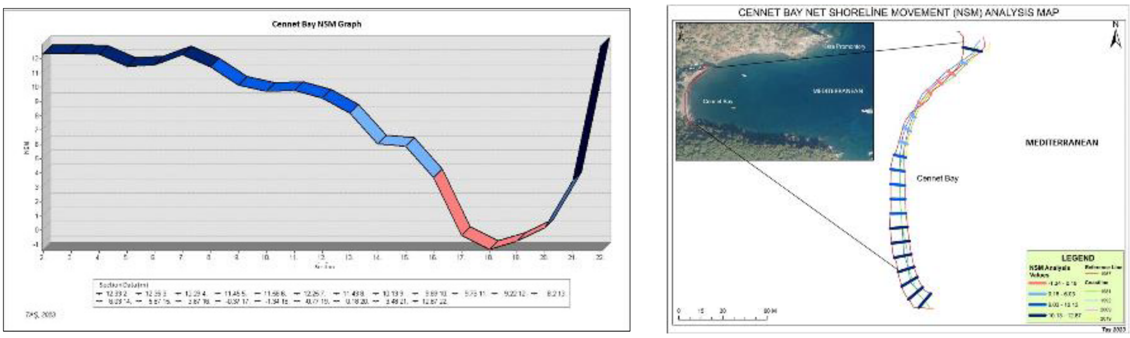

Fig. 18a-b. Cennet Bay NSM graph (a). Cennet Bay NSM map (b).

Cennet Bay EPR Analysis Results

In the EPR analysis of Cennet Bay, data was collected from 21 points at 10-meter intervals. Over the 62-year period between 1957 and 2019, the most substantial accumulation was recorded in section 21, with an accumulation rate of 0.21 meters per year (Fig. 19a-b). The regions where sections 1, 2, and 3, passing through the southern part of Cennet Bay, are situated, are also notable for their high accumulation rates. During the period from 1957 to 2019, the highest erosion rate was observed in the vicinity of section 17, with a rate of -0.02. Cennet Bay, overall, has experienced minimal erosion (Fig. 19a-b).

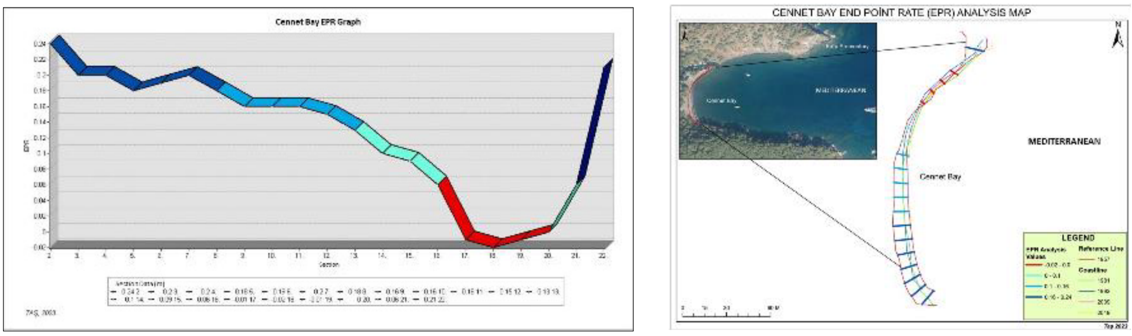

Fig. 19a-b. Cennet Bay EPR graph (a). Cennet Bay EPR map (b).

Cennet Bay SCE Analysis Results

In Cennet Bay, data was collected from 21 points at 10-meter intervals for the SCE analysis. Upon conducting the statistical evaluation of coastlines from various time periods, it was established that the most significant change took place in section 21, amounting to 12.87 meters. Notably, the region where section 21 is located has undergone continuous accumulation over the 62-year period spanning from 1957 to 2019 (Fig. 20a-b).

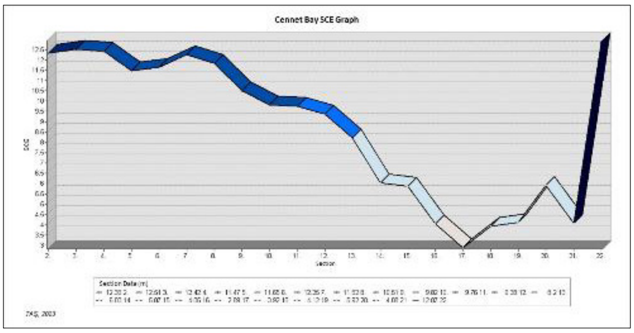

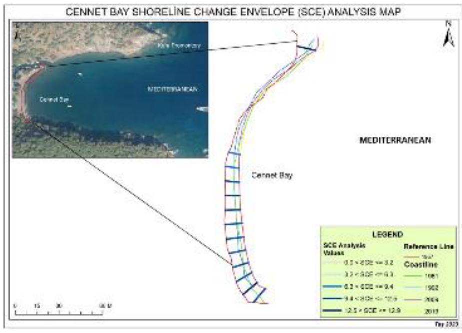

Fig. 20a-b. Cennet Bay SCE graph (a). Cennet Bay SCE map (b).

Results and Discussion

According to the NSM analysis conducted along the coast of Bostanlık Bay (Section A), section 32 experienced an accumulation of 18.97 meters between 1957 and 2019 (Fig. 6a-b). However, in the SCE analysis for Bostanlık Bay (Section A), the area where section 32 is situated endured an erosion of -10.27 meters from 1981 to 1992, followed by a significant accumulation of 27.11 meters from 1992 to 2019 (Fig. 8a-b). The primary driver behind this accumulation is the sediment carried by the Karaçay Stream. The Karaçay Stream rapidly reaches the sea shortly after its source, and due to its valley being established in a steeply inclined area, it contributes to the presence of coarse-grained pebbles along the shores in this region. Today, human interventions have reinforced the shoreline with rocks to combat erosion.

In the NSM analysis conducted along the coast of Bostanlık Bay (Section B), a comparison of 1957 and 2019 data revealed accumulation on the 590-meter-long shore located to the south of the cliff formed by the rocks of Çöğmen Tepe, with an increase of 7.22 meters documented in section number 25. In contrast, the shores north of the 750-meter-long cliff where the port is situated experienced erosion, resulting in a decrease of -17.57 meters in section 124. Remarkably, minimal change was observed in the vicinity of the cliff itself (Fig. 9a-b).When comparing data from 1957 to 2019, it is evident that there was accumulation on the southern shores of Bostanlık Bay (Section B). However, from 1992 onwards, erosion began affecting the coasts in this area. Notably, this area features a transition from coarse gravel alluviums to coarse sandy materials brought by the Karaçay Stream. Erosion has persisted in the northern part of the cliff since 1957. The primary reason behind the consistent erosion in this area is its vulnerability to waves and currents. The presence of thin dunes along the coasts in this area has further exacerbated the impact of wave erosion.

The analysis of the City Port, which encompasses coarse dunes and extends over a length of 235 meters, predominantly revealed accumulation, with erosion detected in a limited section of the northern shores. The primary factor contributing to accumulation in this area is the City Port's location within a small bay, where the impact of waves and currents is relatively less pronounced.In line with the NSM analysis, a comparison between 1957 and 2019 data indicated an accumulation of 10.31 meters in section number 8. On the northern side of the City Port, an erosion of -4.55 meters was observed (Fig. 12a-b). It's worth noting that the breakwaters that were once present in this area have now been submerged, likely due to the tectonic characteristics of the region.

The North Port, situated to the north of the tombolo, extends over a length of 590 meters. This port is located within an open bay characterized by coarse sand. Accumulation in the southern part of the North Port is primarily attributed to seasonal streams originating from Tahtalı Mountain. Furthermore, the southern section of the North Port, nestled within the valley of the Asar Tombolo, benefits from a more sheltered position against the impact of waves and currents compared to the northern part. The results of the analyses conducted in the North Port demonstrate a pattern where accumulation prevails in the southern sections of the North Port, with an increase of 11.79 meters observed in section number 2. In contrast, the northern parts of the North Port exhibit a dominant erosion trend, resulting in a decrease of -11.12 meters documented in section number 55 (Fig. 15a-b).

The analyses conducted in Cennet Bay reveal a prevailing pattern of accumulation across the bay between 1957 and 2019, with a remarkable increase of 12.87 meters noted in section number 21 (Fig. 18a-b). The primary contributor to this accumulation in Cennet Bay is the Alacasu Stream, which serves as a seasonal watercourse. As the Alacasu Stream flows into the sea from Cennet Bay, it deposits alluvial materials, creating a pebbly beach in this area. The influence of waves and currents in Cennet Bay, nestled between İnce Promontory and Kara Promontory, is notably minimal. These two capes function as natural protective barriers for the beach, resulting in very limited erosion within Cennet Bay (with the highest erosion recorded at -1.34 meters in section 17). A noteworthy transformation occurred in Cennet Bay when it was converted into a public beach. The excavation material from the construction of a secondary road leading to the beach was deposited at the mouth of the stream. Subsequently, this anthropogenic fill was extended into the sea by local fishermen, creating a sheltered area for fishing activities behind it.

BIBLIOGRAPHY

Akköprü E., E. Berberoğlu & M. Taş 2022, “Phaselis ve Yakın Çevresinin Coğrafi Özellikleri”. *Phaselis* VIII, 223-236.

Aslan E. & Orhan U. 2019, “Phaselis 2018 Yılı Güney Liman Alanı Sualtı Araştırmalarında Tespit Edilen Amphoralar”. *Phaselis* V, 85-99.

Arslan & Tüner Önen 2021, “Phaselis 2021 Yılı Kazı Yüzey Araştırmaları”. *Phaselis* VII, 147-190.

Atasoy L. 2010, *Yat Kaynaklı Atık Suların Phaselis Koyuna Çevresel Etkileri ve Marinalarda Atık Su Yönetimi*. Yayımlanmamış Yüksek Lisans Tezi, Akdeniz Üniversitesi. Antalya.

Dolan R., M. S. Fenster & S. J. Holme 1991, “Temporal Analysis of Shoreline Recession And Accretion”. *Journal of Coastal Research* VII/3, 723-744.

Döker M. F. 2012, “İstanbul İli Marmara Denizi Kıyı Çizgisinde Meydana Gelen Zamansal Değişimin Belirlenmesi”. *International Journal of Human Sciences* IX/2, 1350-1370.

Himmelstoss E. A., A. S. Farris, R. E. Henderson, M. G. Kratzmann, A. Ergul, O. Zhang, J. L. Zichichi & E. R. Thieler 2018, *Digital Shoreline Analysis System (version 5.0): U.S. Geological Survey Software Release*. https://code.usgs.gov/ cch/dsas.

Kılar H. & Çiçek İ. 2018, “Göksu Deltası Kıyı Çizgisi Değişiminin DSAS Aracı ile Belirlenmesi”. *Coğrafi Bilimler Dergisi* 16/1, 89-104.

Kuleli T. 2010, “Kızılırmak ve Yeşilırmak Deltalarındaki Kıyı Değişimlerinin Landsat TM ve DSAS ile Belirlenmesi”. *Türkiye’nin Kıyı ve Deniz Alanları VIII. Ulusal Kongresi*, *27 Nisan- 1 Mayıs, Trabzon*.

Öner F. 2018, “Phaselis Antik Kenti Küçük Hamamı ve Latrina’sında Kullanılan Yapıtaşları ve Bu Yapıtaşların Bozuşmaları”. *Phaselis* IV, 351-360.

Özpolat E. & Demir T. 2014. “Coğrafi Bilgi Sistemleri ve Uzaktan Algılama Yöntemleriyle Kıyı Çizgisi Değişimi Belirleme: Seyhan Deltası”. *Akademik Bilişim* (111-116). Mersin.

Schafer J. 1981, *Phaselis. Beiträge zur Topographie und Geschichte der Stadt und ihrer Häfen* (Ist. Mitt. Beiheft 24). Tübingen.

Topuz M. 2018, “Sarıkum Lagünü (Sinop) Kıyı Çizgisinde Meydana Gelen Değişimlerin Uzaktan Algılama Teknikleriyle İncelenmesi”. *The Journal of Academic Social Science Studies* 71, 481-493.